# Quantum Face Recognition With Multigate Quantum Convolutional Neural Network

Yijie Zhu, Ahmed Bouridane, M Emre Celebi, Debanjan Konar, Plamen Angelov, Qiang Ni, and Richard Jiang

***Abstract*—In the last decade, quantum computing has showcased its unique mechanism across diverse fields, highlighting significant potential for data-driven applications requiring substantial computational resources. Within this landscape, quantum machine learning emerges as a promising frontier, poised to harness the unique advantages of quantum computing for machine learning tasks. Nonetheless, the current generation of quantum hardware, typified by noisy intermediate-scale quantum (NISQ) devices, grapples with severe resource constraints, particularly in terms of qubit availability. While quantum computing offers tantalizing capabilities such as superposition and entanglement, which can be strategically leveraged to optimize the performance of quantum neural networks, the challenge remains in mitigating the resource limitations while upholding high recognition accuracy. To address this imperative, we introduce a pioneering face recognition method christened the multigate quantum convolutional neural network (MG-QCNN). This innovation is engineered to surmount the resource bottleneck endemic to NISQ devices while preserving exceptional recognition accuracy. Our empirical investigations conducted on benchmark datasets, including the Yale face dataset and the ORL face database, illuminate the remarkable potential of this approach. Specifically, our proposed variational quantum circuit architecture consistently achieves an impressive average accuracy of 96%, which is better than the 95% of the classic CNN. Our model underscores the efficacy of quantum convolution operations in the extraction of feature maps, exhibiting a transformative stride toward unlocking the full potential of quantum-enhanced face recognition, and compared with other quantum models, our method has more advantages in accuracy and efficiency.**

***Impact Statement*—Our groundbreaking research in quantum machine learning has unveiled a transformative path forward in the realm of face recognition. By pioneering the multigate quantum convolutional neural network, we have harnessed the unique capabilities of quantum computing to overcome resource limitations and achieve an astounding 96% average accuracy on face recognition tasks. This achievement not only showcases the immediate potential of quantum convolution operations in feature extraction but also sets the stage for a quantum revolution in the field of machine learning. Our work is a catalyst for future explorations, promising even greater computational efficiency and accuracy as we scale up quantum structures and expand our horizons to high-resolution color face images. This study is a foundational step toward quantum-enhanced face recognition, with far-reaching implications for data-driven applications and the broader field of artificial intelligence.**

***Index Terms*—Multigate quantum convolutional neural network (QCNN), quantum biometrics, quantum convolutional neural network (QCNN), quantum machine learning.**

## I. Introduction

FACE recognition, a biometric technology for identity recognition [1], finds valuable applications in various sectors such as banking, security, and government [2]. The process of facial recognition encompasses several stages, including face image acquisition, image preprocessing, facial feature extraction, and image recognition [2]. Among these stages, the extraction and modeling of facial features stand as a pivotal step. By modeling these features from the facial image, we can subsequently employ them to match and determine the identity of the individual [2].

Among the methods of facial feature extraction, the most widely used methods are machine learning, such as K-nearest neighbors (KNN) and support vector machines (SVM) [3]. Backed by the powerful processing power of GPU units, deep learning methods have achieved dominance in this field [35], [36], [37], [38]. Among them, the deep learning method based on convolutional neural network (CNN) is one of the best-performing methods [2]. CNN for computer vision was proposed by LeCun et al. [4]. The advantages of CNN over traditional neural networks lie in its parameter sharing mechanism and the sparsity of connections, which are brought about by its creative use of convolution kernels. CNN has received extensive attention from industry and academia in the past few years due to its impressive achievements in many fields including but not limited to computer vision and natural language processing [5]. DeepFace [6] is the foundation of the application of CNN in face recognition and achieved an accuracy of 97.35% on the LFW dataset [7], which is very close to the human level.

Manuscript received 5 April 2023; revised 6 October 2023, 7 February 2024, and 30 March 2024; accepted 10 June 2024. Date of publication 28 June 2024; date of current version 10 December 2024. This work was supported in part by the UK EPSRC under Grant EP/P009727/1, in part by the Leverhulme Trust under Grant RF-2019-492, and in part by the US National Science Foundation under Grant 1946391. This article was recommended for publication by Associate Editor Aaron Baughman upon evaluation of the reviewers' comments. *(Corresponding author: Richard Jiang.)*

Yijie Zhu, Plamen Angelov, Qiang Ni, and Richard Jiang are with LIRA Center, Lancaster University, LA1 4YW Lancaster, U.K. (e-mail: r.jiang2@lancaster.ac.uk).

Ahmed Bouridane is with the Centre for Data Analytics and Cybersecurity (CDAC), University of Sharjah, Sharjah 27272, UAE.

M Emre Celebi is with the Department of Computer Science, University of Central Arkansas, Conway, AR 72035 USA.

Debanjan Konar is with Purdue Quantum Science and Engineering Institute (PQSEI) and School of Industrial Engineering, Purdue University, West Lafayette, IN 47906 USA.

Digital Object Identifier 10.1109/TAI.2024.3419077

Although deep learning has achieved great success, there are also some problems. The article [43] shows that progress along current routes is rapidly becoming unsustainable economically, technologically, and environmentally. Facing the problem of computing resources, forcibly consuming more resources may not be a good development direction. It's a much better idea to balance efficiency while maintaining great performance.

Compared with classical computing, quantum computing has its unique advantages in the field of machine learning [8]. Applying quantum computing to classical neural networks is one of the major recent application directions of quantum computers [53], [54], [55]. On some problems, quantum mechanisms are expected to perform better than classical algorithms, especially the potential for quantum polynomials through quantum parallelism speed up [8], [47], and many people try to use the properties of quantum computing to improve the efficiency of models. Currently, researchers are primarily concentrating on one of the most captivating facets of quantum computers: quantum parallelism, which relies heavily on the superposition of states and is typically the primary cause of the higher speed of quantum algorithms compared with classic ones. The results of the experiments [12] indicate that it is achievable to take advantage of the parallelization of existing quantum hardware and acquire speed up from it. Currently, the development of quantum computing is in the stage of noisy intermediate-scale quantum (NISQ) with limited performance. While quantum machine learning has achieved some virtuosity [10], quantum-based face recognition is still in a relatively early research stage due to the limitation of the number of qubits in current quantum computers. Take the commonly used LFW face database as an example. The dataset contains 13,000 face images [6]. Even if each face image is reduced to a size of $12 \times 12$ pixels, the demand for the number of qubits still exceeds the processing power of current quantum computers. In addition, the quantum resources currently available are relatively limited and expensive. Due to the structure of the QPU itself, the number of qubits, and the limitations of the quantum volume, the QPU may not be able to meet the researchers' design of a variety of quantum gates and qubits in quantum circuits, including amplitude encoding methods and some classic loss functions. The currently commonly used and affordable IBM QPU has qubits ranging from 5 to 27 qubits, so researchers must ensure that every qubit in their quantum circuits is used as efficiently as possible.

In recent years, face recognition technology, driven by deep learning, has been extensively studied and is one of the most popular research topics in pattern recognition and image processing. The purpose of face recognition is to extract the personalized features of people from face images and use this to identify different people. For example, face recognition based on Gabor filtering [9], face recognition method based on elastic graph matching [6], and method based on fuzzy neural network [11]. At present, various face recognition models based on deep learning have shown excellent performance [44], [45], [46].

In the face recognition model based on a neural network, the CNN structure is one of the most commonly used structures [1]. A CNN is a neural network consisting of neurons with learnable weights and bias constants [2]. For image input, this method can effectively extract local features. This feature of CNN is suitable for data with a strong correlation between pixels such as face images.

Our goal is to realize an easily extensible quantum structure on a limited number of qubits, aiming at better utilization of qubits to achieve higher efficiency. Our results show that only four qubits are required for high-accuracy face recognition on low-level face data.

We propose a trainable quantum convolutional architecture that requires a small number of qubits and can be combined with classical neural networks. Simulation is a viable training option due to the low number of qubits required. Building on previous research, we use a variational quantum algorithm-based convolution method. We designed a new quantum circuit, using a variety of quantum rotation gates to fit the objective function better. Therefore, we name this method as multigate quantum convolutional neural network (MG-QCNN). Our main contributions are:

1) We propose a multigate method for encoding and setting parameters in quantum circuits. This method applies a variety of quantum rotation gates to better fit the objective function.
2) Using quantum entanglement to achieve convolution, all qubits of the quantum circuit are measured in the measurement phase, so that the eigenvalues obtained by convolution can reflect the correlation between pixels in the region.
3) Our method can be viewed as a quantumed convolutional layer and thus can be easily combined with various network structures.
4) Our structure is lightweight, requiring fewer qubits and occupying a small quantum volume, making it easy to deploy in practice. Fixed quantum circuits are more efficient and interpretable than the continuous generation of random circuits.

Overall, our proposed MG-QCNN considers improving efficiency in addition to improving accuracy. Through the analysis and discussion of the experimental results, MG-QCNN achieves the following performance.

1) The proposed MG-QCNN achieves average accuracies of 90% and 91% in two different databases, outperforming previous quantum machine learning methods.
2) The superiority of using quantum entanglement to generate feature maps in quantum convolution kernels is demonstrated, and the correlation between feature maps is strong under the action of quantum entanglement, which is superior to classical CNN operations.
3) Our model training speed and resource consumption are better than existing approaches.
4) Our architecture can be easily combined with classic neural network structure.

The structure of this article is as follows: First, we discuss face recognition and related work in the field of quantum machine learning. Subsequently, we introduce the details of MG-QCNN. After that, we describe the experimental setup and present the experimental results. Finally, we discuss the results of the experiments.

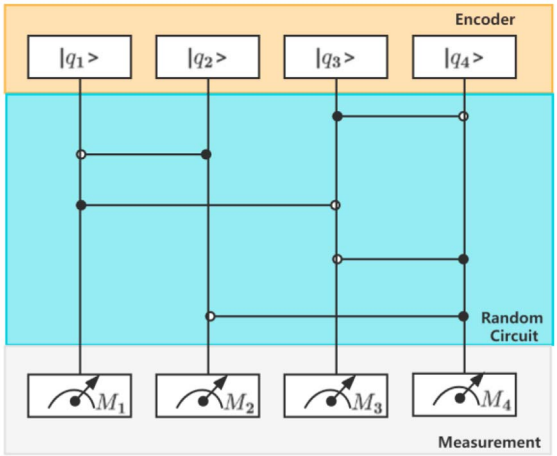


Fig. 1. Quantum circuit of QNN [20]. The quantum circuit in the blue part is a random circuit, that is, the CNOT gates are randomly generated and are different for each training. All qubits will be measured in the measurement section.

## II. Background

### A. Quantum Machine Learning

Mechanisms such as quantum entanglement and superposition state possessed by quantum systems give quantum systems an advantage over classical computers in solving some problems [13]. In machine learning tasks, with the deepening of research, the number of training samples and model parameters continue to increase, and the high parallelism of quantum systems is considered to optimize traditional machine learning. At present, a variety of quantum machine learning methods have been proposed, such as the quantum Boltzmann machine [14] and quantum neural network [15], [16]. A Quantum neural network is a neural network model based on the principles of quantum mechanics. Or the quantum neural network is a deep learning method that introduces quantum circuits into classical neural networks [47]. Ezhov and Ventura [17] discussed various advantages of quantum neural networks over classical neural networks: The information that a single qubit can carry increases exponentially compared with bits [48]; Quantum polynomial speedup [49]; Single-layer network solution of linearly inseparable problems [42]. Recently, Ezhov suggested that quantum neural networks do not need to be based on qubits, and criticized attributing them to quantum machine learning methods or any other method. He argued that quantum neural networks can be seen as a universal tool for representing amplitudes of any quantum process [33].

A quantum circuit is a key part of quantum machine learning systems. A quantum circuit consists of several qubits and quantum gates as shown in Fig. 1. Lines side by side represent the qubits, and from up to bottom represent the chronological order. The vertical lines on these straight lines represent controlled NOT gate (CNOT) gates that are essentially unitary operators. Quantum gates can be applied to one or two qubits. Any unitary transformation acting on any set of qubits can be implemented by a combination of a series of quantum gates. At the end of the line is the measurement section.

### B. Variational Quantum Algorithm

Variational quantum algorithms (VQA) use classical optimizers to train quantum circuits with parameters [18]. For classical deep learning, the model is usually a neural network running on a classical computer. For VQA, the neural network is replaced by a quantum circuit running on a quantum computer. A quantum circuit is a variational quantum circuit (VQC). VQC usually consists of a series of single-qubit gates or multiqubit gate operations. Some VQCs are used in hybrid methods, as a preprocessing or postprocessing part combined with classical methods [19], [34], [53], [54], [55]. Parameters in VQC can be optimized in classical network layers, just like in classical machine learning, which is why VQC is suitable for building hybrid architectures. The parameters in VQC are mainly reflected in the rotational gate in the quantum circuit, and the parameters of its rotation can be trained. VQA optimizes the parameter $\theta$ in the circuit by gradient descent to minimize the cost function. In this way, the parameters of the quantum circuit itself can be updated, enabling wider and more flexible deployment of quantum circuits in neural networks. The cost function of VQA is usually the expected value of the observed object $H$ in the final state of the line, and the formula is as follows:

$$E = \langle 0 \mid U^{\dagger}(\theta) H U(\theta) \mid 0 \rangle. \tag{1}$$

### C. Related Quantum Convolutional Models

Due to the excellent performance of CNN in classical machine learning, a method using full quantum architecture was proposed due to its influence. The QCNN [21] implements the convolutional layer and pooling layer similar to the classical CNN architecture on the quantum circuit and finally determines the final classification result through the fully connected layer.

Quanvolutional neural network (QNN) is a quantum network inspired by classical CNN [20]. Before QNN, a QCNN using the idea of convolution has been proposed [21]. This quantum neural network implements quantum convolution and quantum pooling on quantum neural networks to deal with many-body physics problems. However, this QCNN differs from the classical CNN in that it does not have a structure similar to a convolution kernel (filter). This also means that if QCNNs are applied to face recognition, the requirement for the number of qubits will be huge: one qubit per pixel. This reduces the overall efficiency of the network.

QNN extends the classical CNN structure with quantum quanvolutional layers but does not replace the whole neural network with quantum layers. Similar to classic convolutional layers, quanvolutional layers can adjust the number of quanvolutional kernels (filters) within the layer, and can be placed at any desired position as a completely independent layer when used in a neural network. The filter structure in the quanvolution layer is similar to the filter in CNN and can extract local features. Fig. 1 is the structure of the quanvolutional layer. The quantum circuits that constitute the filter in QNN are random circuits, which are different each time they are generated.

QNN has many advantages. First, the structure of the QNN makes it easy to combine with traditional neural network layers.

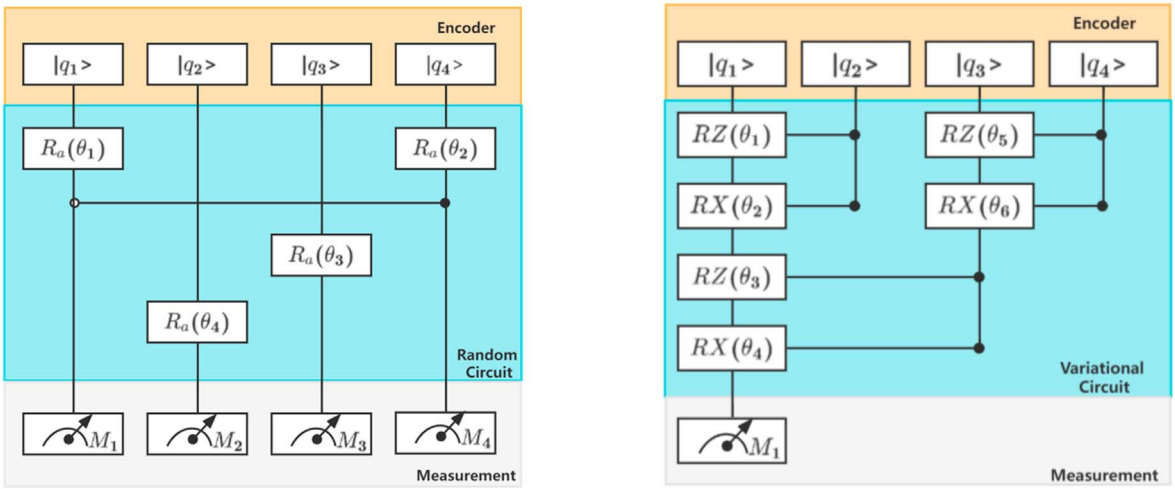


Fig. 2. Left figure is VQNN [19]. The quantum circuit in the blue part is a random circuit, that is, the CNOT gate and the rotation gate are randomly generated, and each training is different. The parameters in the rotation gate are updated via the cost function. In addition to the difference between quantum circuits and quanvolution neural network, the introduction of trainable parameters enables VQNN to be separated from classical CNN and train independently, which is different from QNN which must rely on classical networks. The right figure is QCNN [22]. The quantum circuit is composed of the control $R_Z$ gate and the control $R_X$ gate. Only one qubit is measured during measurement, and multiple quantum convolution kernels are set, making QCNN similar to classical CNN.

However, referring to Aaronson's research, for algorithms that require a large number of quantum measurements, any potential "quantum speedup" will disappear [22]. If the quanvolutional layer is deployed too much, the speed benefits of quantum computing are difficult to achieve. In addition, more layers require more qubits, which seems to negate the benefit of carrying more information in a single qubit. The quanvolutional layer is not constructed by VQC, so the QNN cannot update the parameters in the kernel, which makes it highly dependent on the classic CNN when using this structure to form a neural network, and cannot replace the classic CNN.

Considering that QNN cannot train parameters, an improved structure using VQC, variational quanvolutional neural network (VQNN), is proposed [19]. As the name suggests, this structure changes the quantum circuit into a VQC, adding quantum gates with parameters to the original random circuit. Under the action of the cost function, these parameters will be continuously updated, and the gradient descent will be performed as in the classical neural network. The structure of the VQNN is shown in Fig. 2. On the MNIST dataset [24], the VQNN [19] can achieve an average test accuracy of 0.854, and the overall level is better than the QNN [20] trained without parameters. For VQNN [19], its random quantum circuit needs to be regenerated every time it is called, and the interpretability of the random circuit is somewhat lacking. Its use of a single RY gate does not make full use of the Hilbert space and may be lacking in fitting the target state.

In addition, earlier, an article proposed a quantum CNN structure utilizing VQC [23]. This quantum CNN structure is similar to the first two, but a fixed quantum circuit is designed instead of a random circuit. This structure is shown in the figure. The characteristic of this QCNN is that it only measures one qubit in the measurement step, but uses multiple different quantum convolution kernels for multiple measurements. This approach makes QCNN more similar to the classical CNN approach. [52] proposed a structure similar to VQNN, and a model that adds an additional quantum layer to the classic CNN. The article [50] proposes a QCNN for high-energy physics event classification. The proposed quantum architecture demonstrates the advantage of faster learning than the classic CNN when the number of parameters is similar. The article [41] proposes a quantum neural network model inspired by CNN. This article [39] introduces a hybrid quantum classical CNN that applies quantum computing to extract high-level key features from Earth observation data for classification purposes. Furthermore, the adoption of amplitude encoding techniques reduces the required qubit resources. This article [40] proposes a hybrid quantum classical CNN for surface defect recognition. The method introduces quantum CNN layers, reducing the number of convolutional blocks in the model architecture as well as the required image size.

## III. Our Proposed Multigate Quantum CNN

The structure of MG-QCNN we propose is based on VQC, which encodes the image data in the form of classical data, and obtains the expected value through measurement after VQC processing to achieve the function of extracting image features. For face recognition tasks, it is important to exploit the spatial information between pixels. For classical deep learning, merging local pixel regions is an important task, while CNN uses a filter, or convolution kernel, to slide on the original data, collect the values in a rectangular region, and compare the parameters of the filter with the filter. Calculations are made to obtain the eigenvalues of this region. Our proposed method also follows this approach, preserving the 2-D shape of the original image, sliding over the image through a $2 \times 2$ square filter, and encoding the corresponding pixel values onto qubits.

In our multigate approach, we use multiple quantum rotation gates to encode and set parameters. Our method utilizes $R_Y$ gates

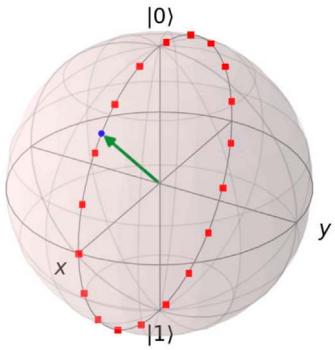


Fig. 3. Figure shows the Bloch sphere. When preparing a quantum circuit, the initial state of the circuit is $|0\rangle$, which is the top of the $Z$-axis. We use an $R_Y$ gate for encoding, so the initial state $|0\rangle$ will rotate around the $Y$-axis. The encoded data will be distributed on the circle as shown by the red square in the figure. The green arrow in the figure and the blue dot points to indicate that the initial state $|0\rangle$ rotates $\pi/4$ around the $Y$-axis.

to encode the pixels of the raw data, transforming classical data into quantum data on qubits, and rotates each qubit using $R_X$ and $R_Z$ gates that carry parameters. With the calculation of the loss function, the parameters of the $R_X$ gate and the $R_Z$ gate are continuously updated, so that the model is fitted to the objective function. Our method can theoretically converge better.

When designing a VQC-based quantum convolution structure, there are three main modules to consider: encoder, variational circuit, and decoder.

### A. Encoder

The main function of the encoder is to quantify the input classical data into quantum data that can be input into a quantum circuit. At present, the commonly used coding methods include basic coding, amplitude coding and angle encoding. Angle encoding uses rotation gates to encode classical information, and the rotation angle of these rotation gates is determined by classical information. As shown in the encoder section in Figs. 1 and 2, amplitude encoding is usually achieved by rotating quantum gates. Taking the single-qubit rotation gate as an example, the rotation gate needs to input a rotation parameter. On the Bloch sphere, the state of the qubit will migrate according to the type and parameter of the rotation gate. In our architecture, $R_Y$ gates will be used for all classical data, and each qubit carries one data (i.e. one pixel in the original image). We first normalize the raw data to unit length before entering the $R_Y$ gate as a parameter. The initial state of all our qubits is $|0\rangle$, rendered on a Bloch sphere as shown in Fig. 3. As we use the $R_Y$ gate encoding, the state of the qubit embodied on the Bloch sphere is rotated from the initial state $|0\rangle$ around the $Y$-axis according to the parameter $\theta$. We choose the $R_Y$ gate because the rotation of the initial state along the $Y$-axis can most intuitively reflect the original data in the quantum system. The equation for encoding using the $R_Y$ gate is as follows:

$$R_y(\phi) = e^{-\frac{i\phi\sigma_y}{2}} = \begin{bmatrix} \cos\left(\frac{\phi}{2}\right) & -\sin\left(\frac{\phi}{2}\right) \\ \sin\left(\frac{\phi}{2}\right) & \cos\left(\frac{\phi}{2}\right) \end{bmatrix}. \tag{2}$$

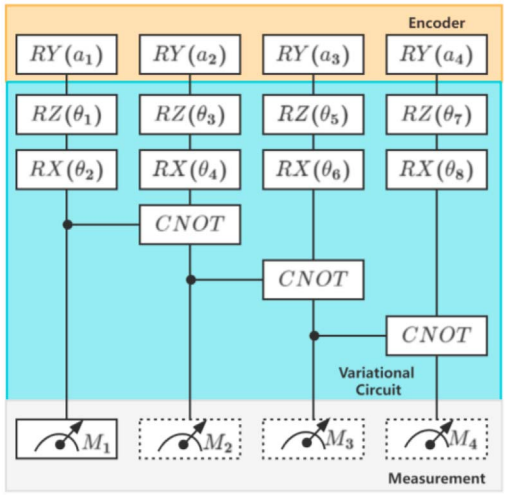


Fig. 4. Quantum circuit of MG-QCNN. The dashed lines in the measurement section represent whether or not measurements were made here in the different models. Our model is encoded using $R_Y$ gates, using $R_X$ gates and $R_Z$ gates to carry a total of eight parameters, two on each qubit. CNOT gates are used to generate quantum entanglement to achieve an effect similar to convolution in classical CNNs.

### B. Variational Quantum Circuit

In this part, the encoded quantum data will be processed by quantum gates. In VQC, rotating quantum gates are often used as carriers of trainable parameters, such as the circuit part in Fig. 2. CNOT gates and control revolving gates are used to create quantum entanglement, which is one way of implementing quantum convolutional circuits. The role of this part is to extract data features.

Unlike VQNNs, we design a VQC with a fixed structure, as shown in Fig. 4, rather than a randomly generated circuit. The random circuit will make the result of each training not fixed, and the randomness is very strong. If the VQC is too random, due to their expressibility, a "barren plateau" effect occurs, making model training difficult [25], [51]. This effect can be mitigated using fixed quantum circuits. We use $R_X$ gates and $R_Z$ gates in the circuit to carry trainable parameters, which are the rotation gates around the $X$ and $Z$ axis [56]. We rotate the state along the $y$-axis on the Bloch sphere from the initial state $|0\rangle$ using the $R_Y$ gate in the encoding phase. To make the circuit easier to fit, we deploy $R_X$ gates and $R_Z$ gates on each qubit so that the entire quantum space can be utilized.

Due to the eight quantum rotation gates, our filter carries eight parameters. To improve efficiency, these eight parameters will not change when sliding, which means that the parameters of each $2 \times 2$ area in an image are the same. Although different sets of parameters can be used, we adopt the same set of parameters for the efficiency of the method. The unitary operation of our quantum circuit with an encoder can be expressed by the following equation:

$$U = R_Y(x)R_X(\theta_1)R_Z(\theta_2) = e^{ix\sigma_y}e^{i\theta_1\sigma_x}e^{i\theta_2\sigma_z} \tag{3}$$

where $\theta$ is the parameters and the $x$ is the input data.

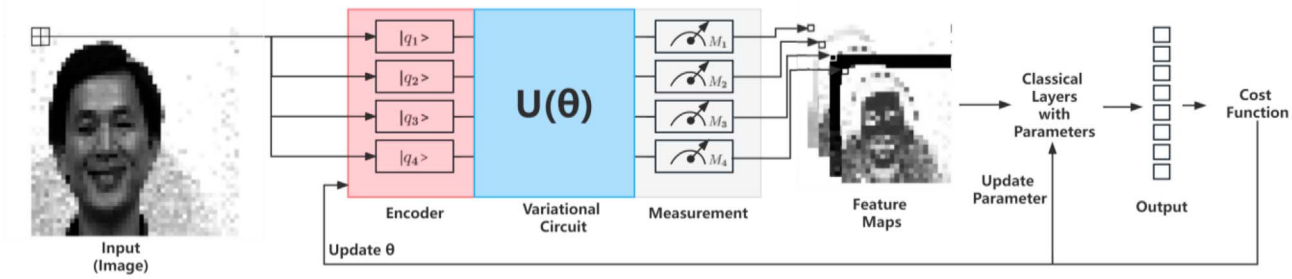


Fig. 5. Figure shows the overall structure of the model in the experiment. The original image is encoded into the quantum circuit with a 2 × 2 area and a stride of 2. U($\theta$) represents a unitary operation consisting of quantum gates. For our MGQCNN, it is a unitary operation composed of $R_X$ gate and $R_Z$ gate, each gate contains one parameter, a total of 8 as shown in Fig. 4 above. After different measurement methods, 24 × 24 × 4 feature maps are obtained, the classic fully connected layer is used for classification, and the parameter $\theta$ is updated after cost function. The model approaches the target after many iterations.

For classic models, there is a universal approximation theorem (UAT) [57] to support its approximation capabilities. Similarly, for quantum models, UAT can be used to demonstrate approximation capabilities. According to [58], a quantum analog can be constructed on the basis of UAT. For any function $g : \chi \to \mathbb{R}$ and for any $\varepsilon > 0$, there exist $n \in \mathbb{N}$ and $w \in \mathbb{R}$ such that

$$\left|\omega\psi_n(x) - g(x)\right| < \varepsilon. \tag{4}$$

For all $x$ in $\chi$ and $\psi_n(x)$ is the basis function. Based on quantum UAT, we can think that our quantum circuits can fit the functions.

### C. Decoder

In the decoder, the processed quantum features will be measured with the help of Pauli Z gates. The expected value of each qubit will be derived from repeated measurements. Through the decoder, the quantum data is converted into classical data, and the classical data can be used as the input for the next layer to continue processing.

Here we consider two cases, measuring all qubits and measuring one qubit but setting multiple convolution kernels. Both measurements have their potential advantages. Measuring a single qubit but setting up multiple convolution kernels makes the quantum convolution layer more similar to the classical convolution operation, but the number of qubits required grows exponentially, as does the number of parameters, which may increase the training time. We will test both measures in experiments to analyze their impact on the overall performance of the model.

After a convolution operation with quantum filters, we obtain a set of feature maps of the original images. Since our quantum architecture is easy to expand, classical neural networks or quantum neural networks can be used to continue processing and further extract features. However, in this study, since our goal is to verify the performance of our architecture, we do not extend the network deeper. Keeping the model structure simple allows us to better analyze the experimental results. We directly feed the resulting feature map into a classical fully connected layer for classification. Through the cost function, the model can update the parameters on the eight quantum rotation gates in the variational quantum circuit. By repeating this process many times, the parameters are continuously updated, and the model is continuously fitted to the objective function we need.

## IV. Experimental Setup And Result Evaluation

In this section, we present our experiments using the method described in the previous section, where the results obtained will be analyzed. Our first experiment will use the Yale Face Database [26], a small database. Due to the limitations of current QML simulation algorithms, it is difficult for us to use large databases, and we think using Yale Face Database is a suitable challenge to demonstrate the lowest performance bounds for systems using minimal parameters. After this, as an increase in difficulty, our experiments will use the ORL face dataset [27]. The ORL face dataset has more data than the Yale Face Database, which is more challenging for our method. We believe that the application of our method to studies on small databases is valuable for its further potential application in medicine.

### A. Experimental Setup

We choose the Yale face database [26] and the ORL database of faces [27] as the experimental data. The Yale face dataset was created by Yale University and contains 15 people, each of whom has 11 face images with different expressions, poses and lighting: center-light, w/glasses, happy, left-light, w/no glasses, normal, right-light, sad, sleepy, surprised, and wink. In a total of 165 images, the original size of each image is 320 × 243 pixels. The ORL database of faces contains a set of images of human faces taken in the laboratory. Each of the 40 different subjects had ten different images, varying lighting, facial expressions (eyes open/closed, smiling/not smiling), and facial details (with/without glasses). The size of each image is 92 × 112 pixels, and each pixel has 256 gray levels.

In this experiment, we test five methods: our proposed MG-QCNN, VQNN [19], HQNN [52], HQCCNN [50], and QCNN [23]. Fig. 5 illustrates the basic architecture of the MG-QCNN. It consists of a VQC layer with one filter and a fully-connected layer with 15 classes. The input data is a 48 × 48 face image. The kernel size and stride of the VQC layer are chosen to be 2 × 2 and 2, respectively. An input image of 48 × 48 pixels is encoded into a four-qubit state using the $R_Y$ rotation gate and then entangled through a CNOT gate with trainable parameters. The decoding part is designed in two ways: either all qubits are measured or only one qubit is measured but with four convolution kernels. The quantum convolutional layer will thus extract a 24 × 24 × 4 feature tensor from the 48 × 48

TABLE I
TEST RESULT OF THE MODELS WITH YALE AND ORL DATA SETS

| | TEST LOSS | | MEAN ACCURACY | | MAX ACCURACY | | RUNNING TIME | | MEMORY | |
|---|---|---|---|---|---|---|---|---|---|---|
| **DATASETS** | Yale | ORL | Yale | ORL | Yale | ORL | Yale | ORL | Yale | ORL |
| **CLASSIC-CNN** | - | - | 93.333% | 94.976% | 95.556% | 96.667% | - | - | - | - |
| **VQNN [19]** | 0.398 | 0.456 | 91.111% | 90.841% | 93.333% | 92.500 | 41256s | 123664s | 6.849GB | 6.854GB |
| **HQNN [52]** | 0.368 | 0.339 | 88.889% | 88.472% | 91.111% | 91.667 | 34165s | 81920s | 3.910GB | 5.272GB |
| **HQCCNN [50]** | 0.385 | 0.362 | 92.775% | 93.267% | 93.333 | 94.167 | 124058s | 342587s | 14.871GB | 19.204GB |
| **QCNN [23]** | 0.384 | 0.336 | 93.333% | 95.097% | 95.556% | **97.500** | 96825s | 236937s | 9.231GB | 12.251GB |
| **MG-QCNN-ALL** | **0.347** | **0.307** | **96.000%** | **95.959%** | **97.778%** | 96.667 | **29567s** | **69169s** | **3.837GB** | **5.086GB** |

pixels input image, which will then be converted into 15 output classes for the Yale Face Database or 40 output classes for the ORL face dataset for different person by the fully-connected layer. A classical CNN that exactly corresponds to the quantum convolutional layer is set as a control. Except that the convolutional layer is classical, other parameters are completely consistent with the quantum layer.

The VQNN has the same structure as our model; however, it incorporates randomly generated quantum circuits. As demonstrated in Fig. 2, the measurement section will assess all qubits. Each filter is composed of four randomly generated quantum rotation gates, thereby containing four parameters. The HQNN is also set as the same.

The setup for QCNN is largely the same, except a single qubit is measured during the measurement phase, with four quantum convolution kernels in place as depicted in Fig. 2. The filter of HQCCNN is $2 \times 3$, and other settings are the same as QCNN.

For Yale Face Database, we train each model for 30 epochs using the Adam optimizer with 20 mini-batches and a learning rate of 0.0001. About 120 images are used for training and 45 images are used for testing. We use cross-entropy as the loss function. For the ORL Database of Faces, we change the learning rate to 0.001. The data is divided into the training set and test set according to the ratio of 7:3. We randomly repartitioned the data set each time we repeated the experiment. Other than these, the other settings are the same.

To conduct a more in-depth analysis of our method, we set up experiments in which the structure of the model was adjusted. We expanded the convolution kernel of the model to $3 \times 3$ for testing. In addition, we also removed the $R_X$ gate and $R_Z$ gate of the model respectively to test the contribution of different quantum gates in the quantum circuit. We also cancel the entanglement in the quantum circuits to test the ability of quantum entanglement to extract data correlations.

We use PennyLane [28] and PyTorch [29] to perform experiments on a local computer with an 8-core CPU 64G memory. PennyLane is an open-source python-based framework that enables automatic differentiation of hybrid quantum-classical computations. It is compatible with mainstream machine learning frameworks like TensorFlow [30] and PyTorch and has a huge plugin ecosystem. In the experiment, we train all models using the built-in Pennylane simulator default_qubit, which supports the backpropagation method of the PyTorch interface. This is a Python-based qubit state vector simulator, with backends written using NumPy, TensorFlow, PyTorch, and JAX. As a result, this simulator supports end-to-end backpropagation, and models containing this device can be deployed for execution on GPUs and TPUs.

Before inputting the data to the model, we normalized the data with a Gaussian distribution, normalized the pixels of the original data to the interval $[-1, 1]$, and then multiplied by $\pi$ as the angle parameter of the RY gate for encoding. The parameters in each quantum filter are initially randomly generated.

Number of shots means how many times an algorithm is run to get a probability distribution of results. Generally speaking for quantum computing, the more measurements, the more accurate the results. However, more measurements mean more quantum resources and time are consumed. To balance the two, we set the number of shots in this experiment to 1000.

### B. Result Evaluation

Table I presents the test results of the quantum models on two datasets. From the results, we found that the MGQCNN-All model achieved the best performance in the five indicators of test loss, mean accuracy, max accuracy, running time, and memory usage. On the Yale dataset, the MG-QCNN-All model achieves a test loss of 0.347, which is better than the QHNN model. The mean accuracy of the MG-QCNN-All model reaches 96.000%, which is 2.667% higher than the Q CNN model with the second highest mean accuracy. For max accuracy, the MG-QCNN-All model achieves 97.778%, which is 2.222% higher than the second. About 93.3% for the VQNN model and MGQCNN-Single model. Meanwhile, the MG-QCNN-All model shows great advantages in training time and memory usage. Compared with the HQNN model, which takes 34 165 s, the MG-QCNN-All model takes 29 567 s, which is 4598 s faster, with a significant time advantage. The time taken by the QCNN model is more than three times that of MG-QCNN-All, and the gap is significant. In terms of memory usage, the MG-QCNN-All model is the least, and the QCNN and HQCCNN models are significantly more than the other models. At the same time, the MG-QCNN-All model shows great advantages in training time and memory usage. Judging from the change curve of loss and accuracy in the training phase in Fig. 6, the QCNN model shows obvious advantages in terms of convergence speed and final loss, but the results in the test are not very good.

For the ORL dataset, from Table I, we find that the MG-QCNN-All model achieves the best performance in terms of test loss, average accuracy, running time, and memory footprint, but the maximum accuracy is that QCNN achieves the best

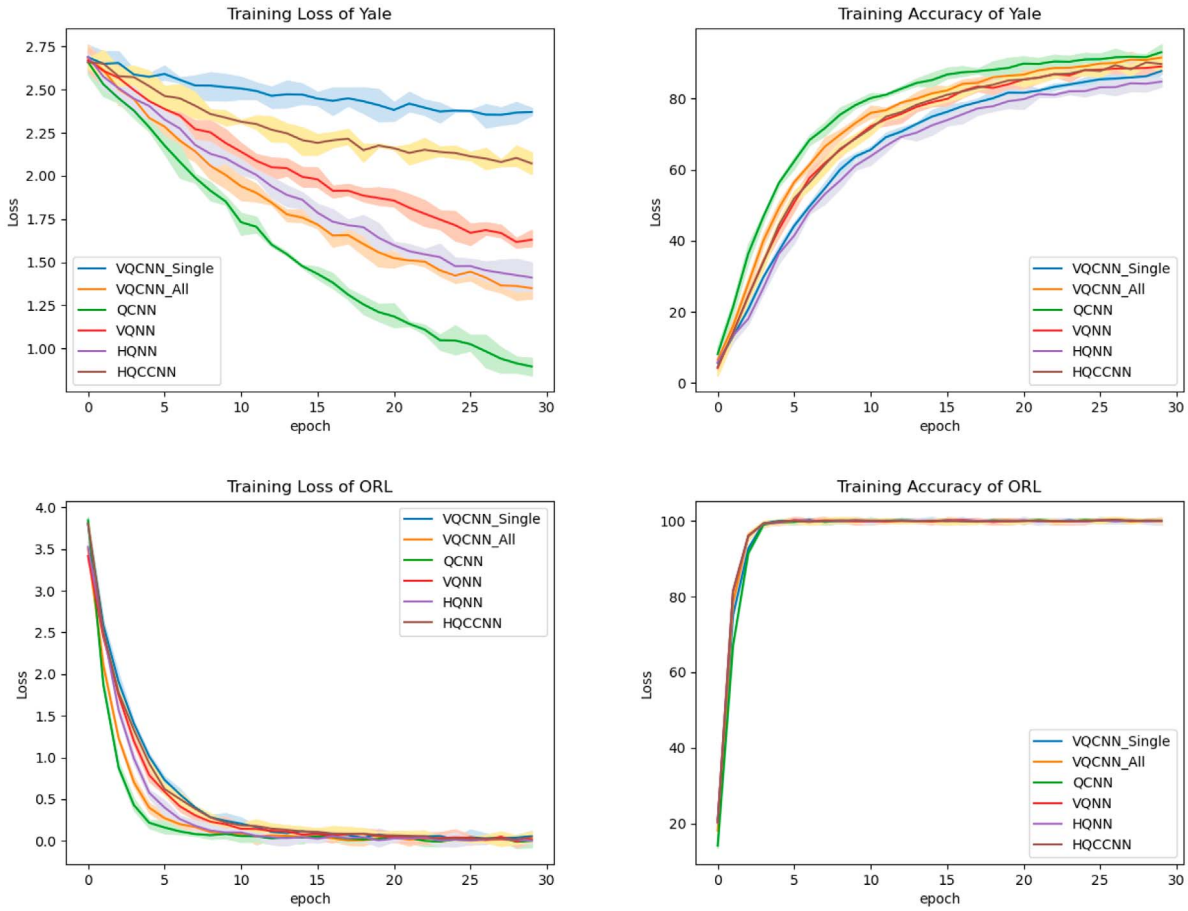


Fig. 6. Upper part is the training loss and accuracy of the models in Yale face database. The lower part is the training loss and accuracy of the models in ORL database of faces.

TABLE II
TEST RESULT OF THE MODELS WITH THE DIFFERENT MEASUREMENT METHODS

| | TEST LOSS | | MEAN ACCURACY | | MAX ACCURACY | | RUNNING TIME | | MEMORY | |
|---|---|---|---|---|---|---|---|---|---|---|
| **DATASETS** | Yale | ORL | Yale | ORL | Yale | ORL | Yale | ORL | Yale | ORL |
| **MG-QCNN-ALL** | 0.347 | 0.307 | 96.000% | 95.959% | 97.778% | 96.667 | 29567s | 69169s | 3.837GB | 5.086GB |
| **MG-QCNN-SINGLE** | 0.412 | 0.531 | 90.222% | 88.573% | 93.333% | 90.833 | 155043s | 254161s | 12.906GB | 15.347GB |

performance. The MG-QCNN-All model achieves a test loss of 0.307, outperforming the QCNN model. The average accuracy of the MG-QCNN-All model reaches 95.959%, which is 0.862% higher than the second-ranked QCNN model. For the maximum accuracy, the QCNN model reaches 97.5%, which is 0.833% higher than the MG-QCNN-All model. In terms of training time and memory usage, the MG-QCNN-All model still shows its advantages. Compared with the HQNN model, which took 81 920 s, the MG-QCNN-All model took 69 169 s, which was 12 751 s faster, and the time advantage was nearly double. The QCNN model took 236 937 s. This time is four times that of MG-QCNN-All, and the difference is significant. It can also be seen from the memory usage of the model that the number of parameters has a huge impact on the resource consumption of model training. Judging from the change curves of loss and accuracy in the training phase in Fig. 6, the QCNN model still shows advantages in terms of convergence speed and final loss, and the average accuracy in the test results is still not as good as the MG-QCNN.

We modified the measurement part of our model by introducing four convolution kernels, each of which measured one qubit similar to a classic CNN to conduct verification experiments. This experiment allowed us to compare the performance and efficiency of two different measurement methods in the model to determine which one was more suitable for real-world applications. The results of our model on two datasets with two measurements can be seen in Table II. The results indicate that the MG-QCNN-All model performs better in terms of average accuracy, maximum accuracy, running time, and memory.

It can be seen from the results in Table II that the MG-QCNN-All model has higher recognition accuracy. In particular, the average accuracy of the MG-QCNN-All model shows the

TABLE III
TEST RESULT OF THE MODELS WITH THE DIFFERENT STRUCTURES

| | TEST LOSS | | MEAN ACCURACY | | MAX ACCURACY | | RUNNING TIME | | MEMORY | |
|---|---|---|---|---|---|---|---|---|---|---|
| **DATASETS** | Yale | ORL | Yale | ORL | Yale | ORL | Yale | ORL | Yale | ORL |
| **MG-QCNN-ALL** | 0.347 | 0.307 | 96.000% | 95.959% | 97.778% | 96.667% | 29567s | 69169s | 3.837GB | 5.086GB |
| **3×3 FLITER** | 0.398 | 0.521 | 93.333% | 92.917% | 97.778% | 96.667% | 56158s | 167732s | 7.663GB | 8.137GB |
| **RX-REDUCTION** | 0.346 | 0.301 | 89.667% | 89.333% | 93.333% | 94.167% | 28423s | 70285s | 3.677GB | 5.011GB |
| **RZ-REDUCTION** | 0.352 | 0.317 | 91.333% | 90.333% | 95.556% | 94.167% | 29016s | 67293s | 3.701GB | 4.863GB |
| **NO-ENTANGLEMENT** | 0.341 | 0.299 | 88.222% | 88.417% | 91.111% | 91.667% | 28774s | 68024s | 3.762GB | 4.882GB |

best performance on both datasets. It takes the least amount of time and consumes the least amount of resources, which has advantages. In addition, for comparison, we also trained a classical CNN on The ORL database of faces, replacing the quantum layer with the classical convolutional layer, and the accuracy reached 95%. Compared with the classical CNN, our proposed MG-QCNN-All model has an accuracy advantage. According to the comparison between the MG-QCNN-All model and the MG-QCNN-Single model, the performance of the MG-QCNN-All model comprehensively exceeds the MG-QCNN-Single model, and the structure similar to the classical CNN does not bring better performance to the quantum model but increases the model training time. This is due to the imitation of the classical CNN structure resulting in a fourfold increase in the parameters of the filter to 32 parameters. With so many parameters, the speed of training will be greatly slowed down. Especially when using Yale Face Database as the dataset, MG-QCNN-Single is difficult to converge. However, the performance of the QCNN model is second only to the MG-QCNN-All model, and it converges faster than the MG-QCNN-All model in the training phase.

The problem of difficulty in training is also reflected in HQCCNN. Its structure is more complex than MGQCNN and it takes up more resources during training. In general, the training phase converges faster, and the model should perform better on the test set. If the model does not perform well, it may be overfitting. Therefore, we changed the learning rate and epoch of training, tried different combinations, and the performance of the model did not improve. We think the reason for this phenomenon is that the number of parameters of the QCNN model is too large, the data we use in the experiment is limited, and the QCNN model cannot fit the data well. However, as the amount of data increases, the training time of the QCNN model increases substantially. Due to our resource limitation, we were unable to train and test models on large datasets. We adopt the quantum neural network in the hope that the mechanism of quantum computing can provide help for the marginal effect problem and improve the efficiency of the neural network. From our experimental results, it does not seem to be a reasonable choice to use a quantum model with a similar structure to the classical CNN. By contrast, the VQNN model, HQNN and the MG-QCNN-All model have obvious advantages in terms of training speed and hardware resource usage. Even with only one filter, the quantum layer can convert the input 2-D image into four feature maps, and output the correlation between the channels of the feature maps under the action of quantum entanglement.

Overall, from the perspective of loss functions, the results of each quantum model in multiple experiments are relatively stable. However, from the perspective of average accuracy and maximum accuracy, the robustness of HQNN's performance is relatively poor. We believe this is due to the fact that HQNN has fewer quantum gates carrying parameters and does not fully cover every qubit. Apart from this, the quantum models exhibit similar robustness and are generally within an acceptable range.

The VQNN model with four parameters per filter is less accurate and takes longer to train than the MG-QCNN-All model with eight parameters per filter. We analyze that this may be because the quantum circuits of the VQNN model are randomly generated. As a result, the VQNN model requires a large number of random circuits to be generated during training, thereby slowing down its training speed. The fixed design circuits of the MG-QCNN-All model, however, eliminate the need for this step and thus improve training efficiency.

Our experimental results for different structural modifications of our method are presented in Table III. Judging from the results, increasing the size of the convolution kernel does not have a positive impact on the experimental results, but instead reduces the efficiency of the model. We believe this is because larger convolution kernels are currently less efficient for existing loss functions and optimization methods, and there are concerns about "barren plateaus" with more qubits. This problem needs to be solved by redesigning the loss function. In the experiment of removing the $R_X$ gate and $R_Z$ gate, the accuracy of the model dropped significantly. Although the required memory and time decreased, this was due to the overall parameter decrease. In comparison, removing the $R_X$ gate causes a greater decrease in accuracy. This is because the $R_X$ gate affects the $Z$-axis in Bloch space, thus affecting the final measurement results. In the experiment of removing quantum entanglement, the accuracy of the model dropped significantly, which proves that the correlation between the data brought by quantum entanglement is very important, which is also reflected in the experiment of the measurement method.

We extract the incorrectly recognized images from our model experiments for analysis. Fig. 7 shows the accuracy results for specific classes in the data set. Relatively speaking, for the Yale data set, there are a large number of shadows in the background of some data, such as subject 08, which has a higher error rate than other images. For the ORL data set, there is little difference in error rates between faces without glasses and those with glasses. However, for subject 31, the reflection of glasses in five images interferes with the model, and the error rates of these

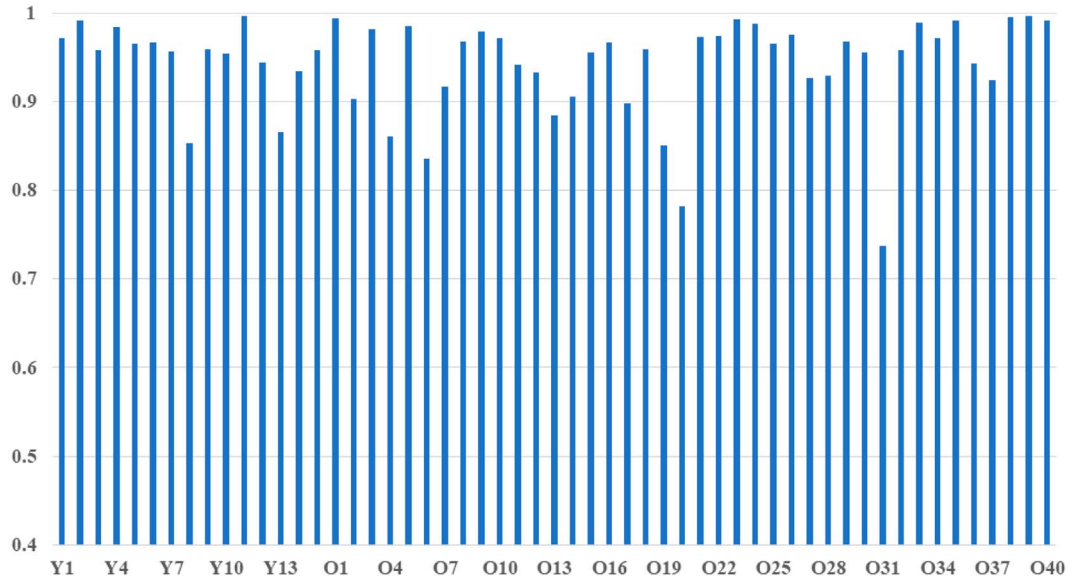


Fig. 7. Accuracy results for different classes of Yale data set and ORL data set. The label Y in the figure represents the Yale data set, O represents the data set, and the following numbers are specific classes.

TABLE IV
THE SETUP OF DIFFERENT QUANTUM CIRCUITS IN THE EXPERIMENT

| | QUANTUM GATES NUMBERS | MEASUREMENT | QUANTUM PARAMETER | RANDOM CIRCUIT |
|---|---|---|---|---|
| **VQNN** | 12 | All | 2,880 | Yes |
| **HQNN** | 11 | All | 2,304 | No |
| **HQCCNN** | 22 | Single | 23,040 | No |
| **QCNN** | 16 | Single | 13,824 | No |
| **MG-QCNN-ALL** | 15 | All | 4,608 | No |
| **MG-QCNN-SINGLE** | 15 | Single | 18,432 | No |

images are relatively high. We believe that these two points are due to the fact that only a single convolutional layer was set up in our experiment, which lacked the ability to extract richer features.

## VI. DISCUSSION

In the previous section, we presented the results of our experiments and analyzed them in detail. Overall, considering the purpose of the research and the experimental environment, the results of our work are good and can provide some methods worthy of reference in the development of related fields.

Although we chose a relatively small data set due to the limitation of the experimental environment, it can be predicted that with the increase in the total number of data and the number of classification classes, the recognition performance of the model will decrease, but our model reaches 95%, in this case. The above mean accuracy can prove the superiority of the model. Similarly, our model structure is relatively simple. Compared with those complex classical neural networks with excellent performance, our quantum network has a low depth and there is a gap in accuracy. However, our quantum model, while simple, is easy to combine our quantum structures with some classical structures, which can be combined with architectures like pooling layers or activation functions in classical CNNs. The parameters and some similarities and differences of each model can be seen in Table IV. The number of parameters mentioned in Table IV is the number of quantum parameters of the model in the Yale dataset. The vast majority of our models are still quantum parameters, and the classical parameters are used to align the classes of the data sets. Taking our experiment as an example, the two data sets are 15 and 40, respectively. We limit the complexity of the architecture. In addition to the limitations of the experimental environment, we want to verify the superiority of our quantum circuits, so keeping the network structure simple is also a reasonable choice.

Extending the size of the quantum convolution kernel is also worth considering. The current reason for limiting the size of a single filter is the "quantum barren plateau" [25]. In general, when there are too many qubits in a VQC-based quantum convolution kernel, the function is too flat and it is difficult to find the minimum value. Although there are ways to alleviate the impact of the "quantum barren plateau", the VQC model with more than 10 qubits can hardly converge, and the $3 \times 3$ quantum convolution kernel is almost the limit. In the future, if VQC cannot make progress on the "quantum barren plateau" problem, quantum convolution methods may have bottlenecks in processing high-resolution single faces. Although there is a "quantum barren plateau" bottleneck, we can also optimize the VQA to achieve high performance with a limited number of qubits as much as possible [31].

Both our proposed quantum neural network approach and encoding method can be implemented and executed on NISQ devices. However, even for small models, learning and inference on quantum simulators are computationally expensive processes. From our experimental results, the time and resources consumed by the training of these simple quantum neural networks are huge compared with classical neural networks, not to

mention that the current quantum simulation cannot use GPU units like classical neural networks, which greatly limits the number of experiments that can be performed. Therefore, quantum convolution methods are currently not suitable for purposes other than research. Furthermore, the quantum simulator we set up is an ideal environment, i.e. a noise-free simulator. Model accuracy is expected to degrade when running on real noisy quantum hardware. However, the model cannot be tested on existing quantum hardware due to the long wait time per image.

In future work, our first consideration is to combine our quantum convolutional layers with some classical neural network structures for better model performance. Increasing the depth of the network, such as the number of quantum convolutional layers, is also a topic worthy of further study. Adding cross-validation to the experiment is also an option worth trying so that we can more fully evaluate the performance of the model. In addition, we will consider expanding on color images, rather than being limited to grayscale images, to better approximate the current classical face recognition task. At the same time, increase experimental data and try to build more complex models.

From our experimental results, quantum computing has the prospect of being applied to practical problems in machine learning like face recognition. Therefore, it is very reasonable to generalize quantum machine learning to other biometrics tasks besides face recognition such as Brain MR and liver tumor segmentation [55], brain tumor segmentation [32], and radiological image classification [34]. Quantum systems have the unique trait of being nonreplicable, which makes them an invaluable asset in the area of biometrics, such as face image data since it significantly reduces the risk of sensitive personal information being leaked. This is helpful for current biometrics privacy [59], [60]. This makes it a valuable area for further research. Quantum computing offers unparalleled security for data due to the fact that measurements of quantum circuits must be taken to gain access to the data, rendering external malicious operations unable to occur without leaving behind a trace. We can introduce a new concept, quantum biometrics, which uses quantum computing to process biometrics, including but not limited to face recognition, fingerprint recognition, iris recognition and a series of image-related tasks, and can also be extended to speech recognition and personal habits. In addition to these routine tasks, the application of quantum methods to genes and proteins is also worth considering the good performance of quantum computing, especially VQA in the field of chemistry.

## VII. Conclusion

In this study, we introduced a novel quantum convolutional model rooted in variational circuits, seamlessly integrating variational quantum circuits and convolutional layers into the framework of quantum neural networks. Our research endeavors encompassed a comprehensive series of experiments involving diverse datasets, yielding a rich tapestry of empirical findings, which we meticulously analyzed. The empirical outcomes unequivocally underscored the advantages of our new model, showcasing its superior computational efficiency and remarkable recognition accuracy. Notably, our investigations revealed that quantum circuits characterized by fixed variation consistently contribute to enhanced model performance.

While the realm of face recognition has been extensively explored within the domain of deep learning, our work represents a pioneering foray into its uncharted territory in the realm of quantum machine learning. As elucidated in our preceding discussions, this study serves as an inaugural stride, laying the foundation for future endeavors in this nascent field. Our future research trajectory will involve the exploration of more expansive datasets and the experimentation with increasingly intricate model architectures, aimed at further refining the classification performance. We are committed to establishing the scalability of quantum structures, seeking to match the prowess of classical neural networks in face recognition tasks. Additionally, the prospect of extending our fundamental methodology to accommodate high-resolution color face images will be a critical avenue for exploration.

## References


[1] I. Adjabi, A. Ouahabi, A. Benzaoui, and A. Taleb-Ahmed, "Past, present, and future of face recognition: A review," *Electronics*, vol. 9, no. 8, 2020, Art. no. 1188.

[2] M. Wang and W. Deng, "Deep face recognition: A survey," *Neurocomputing*, vol. 429, pp. 215–244, Mar. 2021.

[3] P. Parveen and B. Thuraisingham, "Face recognition using multiple classifiers," in *Proc. Int. Conf. Tools Artif. Intell.*, Nov. 2006, pp. 13–15.

[4] Y. LeCun et al., "Backpropagation applied to handwritten zip code recognition," *Neural Comput.*, vol. 1, no. 4, pp. 541–551, 1989.

[5] Z. Li, F. Liu, W. Yang, S. Peng, and J. Zhou, "A survey of convolutional neural networks: analysis, applications, and prospects," *IEEE Trans. Neural Netw. Learn. Syst.*, vol. 33, no. 12, pp. 6999–7019, Dec. 2022, doi: 10.1109/tnnls.2021.3084827.

[6] Y. Taigman, M. Yang, M. A. Ranzato, and L. Wolf, "Deepface: Closing the gap to human-level performance in face verification," in *Proc. IEEE Conf. Comput. Vis. Pattern Recognit.*, 2022, pp. 1701–1708.

[7] G. B. Huang, M. Ramesh, T. Berg, and E. Learned-Miller, "Labeled faces in the wild: a database for studying face recognition in unconstrained environments," Univ. of Massachusetts, Amherst, Tech. Rep., Oct. 2007, pp. 07–49.

[8] L. Alchieri, D. Badalotti, P. Bonardi, and S. Bianco, "An introduction to quantum machine learning: from quantum logic to quantum deep learning," *Quantum Mach. Intell.*, vol. 3, pp. 1–30, Nov. 2021.

[9] R. Hammouche, A. Attia, S. Akhrouf, and Z. Akhtar, "Gabor filter bank with deep autoencoder based face recognition system," *Expert Syst. Appl.*, vol. 197, 2022, Art. no. 116743.

[10] W. O'Quinn and S. Mao, "Quantum machine learning: Recent advances and outlook," *IEEE Wireless Commun.*, vol. 27, no. 3, pp. 126–131, Jun. 2020.

[11] I. F. Iatan, "A fuzzy Kwan–Cai neural network for determining image similarity and for the face recognition," in *Issues in the Use of Neural Networks in Information Retrieval*, Cham, Switzerland: Springer, 2017, pp. 37–79.

[12] L. Mineh and A. Montanaro, "Accelerating the variational quantum eigensolver using parallelism," 2022, *arXiv:2209.03796*.

[13] M. Cerezo, G. Verdon, H. Y. Huang, L. Cincio, and P. J. Coles, "Challenges and opportunities in quantum machine learning," *Nat. Comput. Sci.*, vol. 2, no. 9, pp. 567–576, 2022.

[14] M. Amin, E. Andriyash, J. Rolfe, B. Kulchytskyy, and R. Melko, "Quantum Boltzmann machine," *Phys. Rev. X*, vol. 8, no. 2, pp. 21050–21061, 2018, doi: 10.1103/PhysRevX.8.021050.

[15] Y. Zhang and Q. Ni, "Design of quantum neuron model for quantum neural networks," *Quantum Eng.*, vol. 3, no. 3, p. e75, Sep. 2021.

[16] K. Beer et al., "Training deep quantum neural networks," *Nat. Commun.*, vol. 11, no. 1, pp. 1–6, 2022.

[17] A. Ezhov and D. Ventura, *Future Directions for Intelligent Systems and Information Sciences*. Heidelberg: Physica, 2000, pp. 213–235.

[18] M. Cerezo et al., "Variational quantum algorithms," *Nat. Rev. Phys.*, vol. 3, no. 9, pp. 625–644, 2022.

[19] D. Mattern, D. Martyniuk, H. Willems, F. Bergmann, and A. Paschke, "Variational quanvolutional neural networks with enhanced image encoding," 2021, *arXiv:2106.07327*.
[20] M. Henderson, S. Shakya, S. Pradhan, and T. Cook, "Quanvolutional neural networks: Powering image recognition with quantum circuits," *Quantum Mach. Intell.*, vol. 2, no. 1, 2020.
[21] I. Cong, S. Choi, and M. Lukin, "Quantum convolutional neural networks," *Nat. Phys.*, vol. 15, no. 12, pp. 1273–1278, 2019.
[22] S. Aaronson, "Read the fine print," *Nat. Phys.*, vol. 11, no. 4, pp. 291–293, 2015.
[23] S. Oh, J. Choi, and J. Kim, "A tutorial on quantum convolutional neural networks (QCNN)," in *Proc. Int. Conf. Inf. Commun. Technol. Convergence (ICTC)*, 2020, pp. 236–239, doi: 10.1109/ICTC49870.2020.9289439.
[24] Y. Lecun, L. Bottou, Y. Bengio, and P. Haffner, "Gradient-based learning applied to document recognition," *Proc. IEEE*, vol. 86, no. 11, pp. 2278–2324, 1998.
[25] J. McClean, S. Boixo, V. Smelyanskiy, R. Babbush, and H. Neven, "Barren plateaus in quantum neural network training landscapes," *Nat. Commun.*, vol. 9, no. 1, 2018, Art. no. 4812.
[26] A. S. Georghiades, P. N. Belhumeur, and D. J. Kriegman, "From few to many: generative models for recognition under variable pose and illumination," in *Proc. Fourth IEEE Int. Conf. Autom. Face Gesture Recognit.*, 2000, pp. 277–284, doi: 10.1109/AFGR.2000.840647. [Online]. Available: http://vision.ucsd.edu/content/yale-face-database/
[27] F. S. Samaria and A. C. Harter, "Parameterisation of a stochastic model for human face identification," in *Proc. IEEE Work. Appl. Comput. Vis.*, 1994, pp. 138–142, doi: 10.1109/acv.1994.341300. [Online]. Available: https://cam-orl.co.uk/facedatabase.html
[28] V. Bergholm et al., "PennyLane: Automatic differentiation of hybrid quantum-classical computations," 2018, *arXiv:1811.04968*.
[29] A. Paszke et al., "PyTorch: An imperative style, high-performance deep learning library," in *Proc. Adv. Neural Inf. Process. Syst.*, vol. 32, 2019, pp. 8026–8037.
[30] M. Abadi et al., "TensorFlow: Large-scale machine learning on heterogeneous systems," Softw. Available: Tensorflow.org, 2015.
[31] R. Huang, X. Tan, and Q. Xu, "Learning to learn variational quantum algorithm," *IEEE Trans. Neural Netw. Learn. Syst.*, vol. 34, no. 11, pp. 8430–8440, Nov. 2023, doi: 10.1109/tnnls.2022.3151127.
[32] D. Konar, S. Bhattacharyya, B. Panigrahi, and E. Behrman, "Qutrit-inspired fully self-supervised shallow quantum learning network for brain tumor segmentation," *IEEE Trans. Neural Netw. Learn. Syst.*, vol. 33, no. 11, pp. 6331–6345, Nov. 2022, doi: 10.1109/tnnls.2021.3077188.
[33] A. A. Ezhov, "On quantum neural networks," 2021, *arXiv:2104.07106v1*.
[34] A. Matic, M. Monnet, J. M. Lorenz, B. Schachtner, and T. Messerer, "Quantum-classical convolutional neural networks in radiological image classification," in *Proc. IEEE Int. Conf. Quantum Comput. Eng. (QCE)*, 2022, pp. 56–66.
[35] C. Ashwini and V. Sellam, "Corn disease detection based on deep neural network for substantiating the crop yield," *Math. Inf. Sci.*, vol. 16, no. 3, pp. 423–433, 2022, doi: 10.18576/amis/160304.
[36] M. Zidan, A.-H. Abdel-Aty, A. El-Sadek, E. A. Zanaty, and M. Abdel-Aty, "Low-cost autonomous perceptron neural network inspired by quantum computation," in *Proc. AIP Conf. Proc.*, vol. 1905, no. 1, 2017, Art. no. 020005, doi: 10.1063/1.5012145.
[37] H. H. El-Sayed, S. K. Refaay, S. A. Ali, and M. T. El-Melegy, "Chain based leader selection using neural network in wireless sensor networks protocols," *Appl. Math. Inf. Sci.*, vol. 16, no. 4, pp. 643–653, 2022, doi: 10.18576/amis/160418.
[38] T. M. Shahwan, "A comparison of Bayesian methods and artificial neural networks for forecasting chaotic financial time series," *J. Statist. Appl. Probability*, vol. 1, no. 2, pp. 89–100, 2012.
[39] F. Fan, Y. Shi, T. Guggemos, and X. X. Zhu, "Hybrid quantum-classical convolutional neural network model for image classification," *IEEE Trans. Neural Netw. Learn. Syst.*, early access, doi: 10.1109/TNNLS.2023.3312170.
[40] S. Mishra and C. Y. Tsai, "QSurfNet: A hybrid quantum convolutional neural network for surface defect recognition," *Quantum Inf. Process.*, vol. 22, no. 5, 2023, Art. no. 179.
[41] T. Hur, L. Kim, and D. K. Park, "Quantum convolutional neural network for classical data classification," *Quantum Mach. Intell.*, vol. 4, no. 1, 2022, Art. no. 3.
[42] A.-H. Abdel-Aty, H. Kadry, M. Zidan, E. A. Zanaty, and M. Abdel-Aty, "A quantum classification algorithm for classification incomplete patterns based on entanglement measure," *J. Intell. Fuzzy Syst.*, vol. 38, no. 3, pp. 2817–2822, 2020.
[43] N. C. Thompson, K. Greenewald, K. Lee, and G. F. Manso, "The computational limits of deep learning," 2020, *arXiv:2007.05558*.
[44] M. Kim, A. K. Jain, and X. Liu, "AdaFace: Quality adaptive margin for face recognition," in *Proc. IEEE/CVF Conf. Comput. Vis. Pattern Recognit.*, 2022, pp. 18750–18759.
[45] H. Liu, X. Zhu, Z. Lei, and S. Z. Li, "AdaptiveFace: Adaptive margin and sampling for face recognition," in *Proc. IEEE/CVF Conf. Comput. Vis. Pattern Recognit.*, 2019, pp. 11947–11956.
[46] Y. Zhong, W. Deng, J. Hu, D. Zhao, X. Li, and D. Wen, "SFace: Sigmoid-constrained hypersphere loss for robust face recognition," *IEEE Trans. Image Process.*, vol. 30, pp. 2587–2598, 2021.
[47] Y. Kwak, W. J. Yun, S. Jung, and J. Kim, "Quantum neural networks: Concepts, applications, and challenges," in *Proc. 12th Int. Conf. Ubiquitous Future Netw. (ICUFN)*, 2021, pp. 413–416.
[48] M. Lewenstein, A. Gratsea, A. Riera-Campeny, A. Aloy, V. Kasper, and A. Sanpera, "Storage capacity and learning capability of quantum neural networks," *Quantum Sci. Technol.*, vol. 6, no. 4, 2021, Art. no. 045002.
[49] Z. Zhao, A. Pozas-Kerstjens, P. Rebentrost, and P. Wittek, "Bayesian deep learning on a quantum computer," *Quantum Mach. Intell.*, vol. 1, pp. 41–51, May 2019.
[50] S. Y. C. Chen, T. C. Wei, C. Zhang, H. Yu, and S. Yoo, "Quantum convolutional neural networks for high energy physics data analysis," *Phys. Rev. Res.*, vol. 4, no. 1, 2022, Art. no. 013231.
[51] Z. Holmes, K. Sharma, M. Cerezo, and P. J. Coles, "Connecting ansatz expressibility to gradient magnitudes and barren plateaus," *PRX Quantum*, vol. 3, no. 1, 2022, Art. no. 010313.
[52] A. Senokosov, A. Sedykh, A. Sagingalieva, and A. Melnikov, "Quantum machine learning for image classification," 2023, *arXiv:2304.09224*.
[53] P. Easom-Mccaldin, A. Bouridane, A. Belatreche, and R. Jiang, "On depth, robustness and performance using the data re-uploading single-qubit classifier," *IEEE Access*, vol. 9, pp. 65127–65139, 2021.
[54] P. Easom-McCaldin, A. Bouridane, A. Belatreche, R. Jiang, and S. Al-Maadeed, "Efficient quantum image classification using single qubit encoding," *IEEE Trans. Neural Netw. Learn. Syst.*, vol. 35, no. 2, pp. 1472–1486, Feb. 2024, doi: 10.1109/TNNLS.2022.3179354.
[55] D. Konar, S. Bhattacharyya, T. K. Gandhi, B. K. Panigrahi, and R. Jiang, "3-D quantum-inspired self-supervised tensor network for volumetric segmentation of medical images," *IEEE Trans. Neural Netw. Learn. Syst.*, early access, 2021. doi: 10.1109/TNNLS.2023.3240238.
[56] A. Barenco et al., "Elementary gates for quantum computation," *Phys. Rev. A*, vol. 52, no. 5, 1995, Art. no. 3457.
[57] K. Hornik, "Approximation capabilities of multilayer feedforward networks," *Neural Netw.*, vol. 4, no. 2, pp. 251–257, 1991.
[58] T. Goto, Q. H. Tran, and K. Nakajima, "Universal approximation property of quantum machine learning models in quantum-enhanced feature spaces," *Phys. Rev. Lett.*, vol. 127, no. 9, 2021, Art. no. 090506.
[59] R. Jiang, P. Chazot, N. Pavese, D. Crookes, A. Bouridane, and M. E. Celebi, "Private facial prediagnosis as an edge service for Parkinson's DBS treatment valuation," *IEEE J. Biomed. Health Inform.*, vol. 26, no. 6, pp. 2703–2713, Jun. 2022.
[60] R. Jiang, A. Bouridane, D. Crookes, M. E. Celebi, and H.-L. Wei, "Privacy-protected facial biometric verification using fuzzy forest learning," *IEEE Trans. Fuzzy Syst.*, vol. 24, no. 4, pp. 779–790, Aug. 2016.